Chronocyclic tomography for measuring the amplitude and phase structure of optical pulses

M. Beck and M. G. Raymer

Department of Physics and Chemical Physics Institute, University of Oregon, Eugene, Oregon 97403

I. A. Walmsley and V. Wong

The Institute of Optics, University of Rochester, Rochester, New York 14627

Received July 13, 1993

We describe a new method—chronocyclic tomography—for determining the amplitude and phase structure of a short optical pulse. The technique is based on measurements of the energy spectrum of the pulse after it has passed through a time–frequency-domain imaging system. Tomographic inversion of these measured spectra yields the time–frequency Wigner distribution of the pulse, which uniquely determines the amplitude and phase structure.

There exist several methods for determining the amplitude and phase structure of ultrashort optical pulses.[1–4] All of these involve nonlinear correlation processes and therefore benefit from having pulses of reasonably high peak intensity. Many techniques require the use of deconvolution and/or iterative inversion algorithms, and for some pulses this may lead to ambiguity in reconstructing the electric field.

In related developments, the analogy between temporal pulse shaping [by use of dispersive delay lines (DDL's) and temporal phase modulators] and spatial beam shaping (by use of lenses and spatial propagation), first pointed out by Treacy,[5] was recently developed by Kolner and Nazarathy into the idea of a time lens.[6] In a time lens, a time-dependent optical system focuses ultrashort optical pulses into a narrow time window. Such a system was recently demonstrated by Kauffman *et al.*,[7] who also used it as a time-to-frequency converter for measuring the intensity versus time of an optical pulse without the need for a high-speed photodetector.[8]

Here we point out that, by proper analysis of the data that can be collected by such a time-to-frequency converter system, both the amplitude and the phase structure of an ensemble of optical pulses (or, in principle, a single pulse) can be obtained. This is achieved by use of a tomographic reconstruction method in the time–frequency domain. Because the method directly determines the time–frequency Wigner distribution, we adopt the term chronocyclic, following Paye,[9] and refer to our overall procedure as chronocyclic tomography. An advantage of the method is that it does not require the use of deconvolution and/or iterative inversion algorithms.

To understand how the time–frequency converter may be used to construct the Wigner function, consider a short optical pulse with a complex electric-field envelope $E(t)$ that passes through a DDL (Refs. 5 and 10) and then passes through an rf time-dependent phase modulator.[6] The action of the DDL is to multiply the input field spectrum $\tilde{E}(\omega)$ (Ref. 11) by a frequency-dependent factor $\tilde{G}(\omega) = \exp[-i\phi(\omega)]$. We will approximate the phase factor of the DDL by using $\phi(\omega) = \phi_{\bar{\omega}}'\omega + (1/2)\phi_{\bar{\omega}}''\omega^2$, where $\phi_{\bar{\omega}}'$ is the propagation time of the pulse through the DDL and $\phi_{\bar{\omega}}''$ is the dispersion (the derivatives are evaluated at the pulse center frequency $\omega = \bar{\omega}$). We have dropped the constant term in $\phi(\omega)$ since it corresponds to an unimportant overall phase shift. A grating-based DDL can be well approximated by a quadratic phase shift and can be adjusted to have either positive or negative dispersion.[10]

The temporal phase modulator acts on its input field $E_{\text{in}}(t)$ in the time domain by multiplication with the phase-shift function $M(t) = \exp[i\Phi(t)]$. We will also approximate this phase shift as quadratic, i.e., $\Phi(t) = (1/2)\Phi_{\bar{t}}''(t - \bar{t})^2$, where $\bar{t}$ is the time of zero phase shift and $\Phi_{\bar{t}}''$ is the second derivative of the phase $\Phi(t)$ with respect to (scaled) time evaluated at time $\bar{t}$. Such a phase shift can be approximately generated by using an electro-optic phase modulator driven sinusoidally at rf (gigahertz) frequencies and using a time window near an extremum of the modulation.[7] Because the action of the phase modulator depends on the arrival time of the pulse, it is useful to have a dispersionless delay line that adjust this arrival time. We assume that this delay line cancels the effect of the linear term $\phi_{\bar{\omega}}'$ in the phase of the DDL; this also permits us to take $\bar{t} = 0$.

The spectral function of the field after the temporal modulator is a convolution of the input spectral function with the frequency-domain phase-shift function, given by $\tilde{M}(\omega) \cong (i/\Phi_{\bar{t}}'')^{1/2}\exp(-i\omega^2/2\Phi_{\bar{t}}'')$. The combined action of the DDL and temporal modulator on the field $\tilde{E}(\omega)$ is thus to produce an output spectral function

$$\tilde{E}_{\text{out}}(\omega) = (i/2\pi\Phi_{\bar{t}}'')^{1/2}\exp(-i\omega^2/2\Phi_{\bar{t}}'') \times \int_{-\infty}^{\infty} \exp\{-i[-\omega\omega'/\Phi_{\bar{t}}'' + \frac{1}{2}(\phi_{\bar{\omega}}'' + 1/\Phi_{\bar{t}}'')\omega'^2]\}\tilde{E}(\omega')\mathrm{d}\omega'. \quad (1)$$

Taking ω to be equivalent to the spatial coordinate,

0146-9592/93/232041-03$6.00/0

Eq. (1) has the form of a Fresnel integral describing the passage of an input field through a thin lens and then propagating through free space. Within a phase factor, the Fourier transform of $\tilde{E}(\omega)$ [i.e., $E(t)$] is obtained when terms quadratic in ω' cancel, i.e., when $\phi_{\bar{\omega}}'' + 1/\Phi_{\bar{t}}'' = 0$. Adjusting the magnitude of the temporal phase modulation and measuring the energy spectrum $\langle|\tilde{E}_{\text{out}}(\omega)|^2\rangle$ (where the brackets indicate an ensemble average) by use of a spectrometer and an integrating detector then accomplishes a measurement of the temporal intensity of the input pulse, after proper scaling of the ω variable.[8]

By measuring $\langle|\tilde{E}_{\text{out}}(\omega)|^2\rangle$ at many different values of $\phi_{\bar{\omega}}'' + 1/\Phi_{\bar{t}}''$, one can actually obtain all amplitude and phase information, i.e., $E(t)$, for an ensemble of identical pulses or, in the case of a stochastically fluctuating ensemble, the two-time nonstationary correlation function $C(t,t') = \langle E(t)E^*(t')\rangle$. This is done by use of the chronocyclic Wigner distribution[12]

$$W(\omega,t) = \frac{1}{\pi}\int_{-\infty}^{\infty}\langle E(t+t')E^*(t-t')\rangle\exp(i2\omega t')\mathrm{d}t' \tag{2a}$$

$$= \frac{1}{\pi}\int_{-\infty}^{\infty}\langle E(\omega+\omega')E^*(\omega-\omega')\rangle \times \exp(-i2\omega' t)\mathrm{d}\omega'. \tag{2b}$$

In the case of a reproducible pulse, the ensemble average is dropped here.

Define new variables ω_θ and t_θ, obtained by rotation of ω and t by an angle θ, i.e., $\omega_\theta = \omega\cos\theta + t\sin\theta$ and $t_\theta = -\omega\sin\theta + t\cos\theta$. Integrating the Wigner distribution along a line parallel to the t_θ axis for a fixed value of ω_θ, we get the projected distributions

$$P_\theta(\omega_\theta) = \int_{-\infty}^{\infty} W(\omega_\theta\cos\theta - t_\theta\sin\theta, \omega_\theta\sin\theta + t_\theta\cos\theta)\mathrm{d}t_\theta, \tag{3}$$

each distinguished by a different value of θ. The basis of tomography is that if one can measure the projected functions $P_\theta(\omega_\theta)$ for a sufficient set of values of θ over a π interval, then Eq. (3) can be inverted to obtain $W(\omega,t)$ by use of the inverse Radon transform.[14]

One can obtain the projected functions $P_\theta(\omega_\theta)$ by measuring the spectra $\langle|\tilde{E}_{\text{out}}(\omega)|^2\rangle$ for different values of $\phi_{\bar{\omega}}'' + 1/\Phi_{\bar{t}}''$.[15] This can be seen by insertion of Eq. (2b) into Eq. (3), which yields $P_\theta(\omega_\theta) = \langle|\tilde{\psi}_\theta(\omega_\theta)|^2\rangle$, where

$$\tilde{\psi}_\theta(\omega_\theta) = (2\pi|\sin\theta|)^{-1/2}\int_{-\infty}^{\infty}\exp[-i(\omega_\theta\omega'\csc\theta - \frac{1}{2}\omega'^2\cot\theta)]\tilde{E}(\omega')\mathrm{d}\omega'. \tag{4}$$

This result is similar in form to the output field, given in Eq. (1), of the time–frequency imaging system. The equivalence can be established by choosing the correspondences

$$\cot\theta = -(\phi_{\bar{\omega}}'' + 1/\Phi_{\bar{t}}''), \tag{5a}$$

$$\omega_\theta/\sin\theta = -\omega/\Phi_{\bar{t}}'', \tag{5b}$$

and defining $\tilde{\chi}_\theta(\omega_\theta) = (\Phi_{\bar{t}}''/i|\sin\theta|)^{1/2}\tilde{E}_{\text{out}}[\omega(\omega_\theta)]$, where $\omega(\omega_\theta)$ denotes ω expressed in terms of ω_θ by means of Eq. (5b). With these definitions, $\tilde{\chi}_\theta(\omega_\theta)$ is equal to $\tilde{\psi}_\theta(\omega_\theta)$ in Eq. (4) to within a phase factor, which is not important when only the modulus squared of the spectrum, $\langle|\tilde{\chi}_\theta(\omega_\theta)|^2\rangle = \langle|\tilde{\psi}_\theta(\omega_\theta)|^2\rangle$, is considered. Thus varying $\phi_{\bar{\omega}}'' + 1/\Phi_{\bar{t}}''$ corresponds to rotation in the time–frequency domain, with $\phi_{\bar{\omega}}'' + 1/\Phi_{\bar{t}}'' = 0$ being a rotation by $\pi/2$ (time-to-frequency conversion).

The procedure is as follows: Measure $\langle|\tilde{E}_{\text{out}}(\omega)|^2\rangle$ for different values of $\phi_{\bar{\omega}}'' + 1/\Phi_{\bar{t}}''$, which correspond to different values of rotation angle θ, according to Eq. (5a). Rescale these data to obtain $\langle|\tilde{\psi}_\theta(\omega_\theta)|^2\rangle = P_\theta(\omega_\theta)$ by means of Eqs. (5).[15] Perform the inverse Radon transform on the functions $P_\theta(\omega_\theta)$ to obtain the Wigner distribution $W(\omega,t)$. Invert the Fourier transform in Eq. (2) to obtain the field correlation function in either the frequency or the time domain. In the case of a nonstochastic field, one can factorize the measured correlation function to obtain the complex field structure, up to an unimportant constant phase η_0, i.e., $E(t) = [C(0,0)]^{-1/2}C(t,0)\exp(i\eta_0)$.

From a practical viewpoint, it appears that the apparatus reported in Ref. 8 is adequate for implementing this procedure. To reconstruct the Wigner function it is desirable to cover a range of angles between $-\pi/2$ and $\pi/2$. For a fixed value of $\phi_{\bar{\omega}}''$ we can cover a wide range of angles θ by varying $\Phi_{\bar{t}}''$ from a large negative value to a large positive value, but a small gap in the desired θ coverage occurs. By varying $\Phi_{\bar{t}}''$ from zero to a large positive value and then changing the sign of $\phi_{\bar{\omega}}''$ (i.e., changing the sign of the dispersion in the DDL) and varying $\Phi_{\bar{t}}''$ again, it is possible to cover the full θ range $[-\pi/2, \pi/2]$ without any gap. Using achievable values for the modulator phase shift (48 rad) and frequency (5.2 GHz),[8] and DDL dispersion ($T^2\phi_{\bar{\omega}}'' = \pm 10^7$ fs^2), one can obtain full coverage of θ.

This technique will work for pulses whose durations or bandwidths do not violate the assumptions of quadratic phase shifts in the DDL and the phase modulator. With current technology, the shortest measurable pulse would have a duration of approximately 700 fs; for shorter pulses the required dispersion would stretch the pulse longer than the 30-ps usable window of the phase modulator. For longer pulses the limitations will probably be imposed by the resolution of the spectral measurements.

We have simulated the reconstruction of a coherent two-pulse sequence with linear frequency chirp, with an electric field

$$E(t) \propto \{\exp[-(t-\tau)^2/2] + \exp[-(t+\tau)^2/2]\}\exp(i\gamma t^2). \tag{6}$$

The intensity and the phase of this pulse with values of the parameters $\tau = 2$ and $\gamma = \pi/27$ are plotted

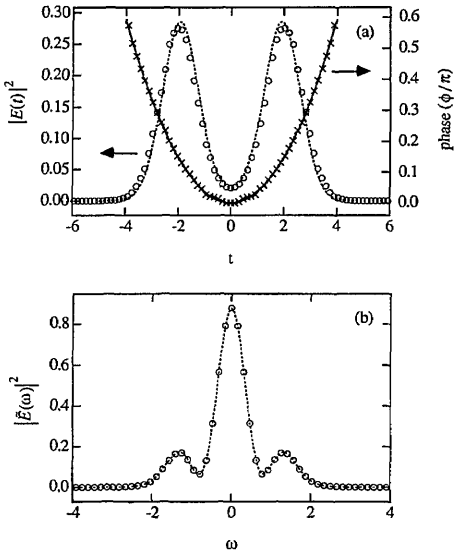

Fig. 1. (a) Pulse intensity $|E(t)|^2$ plotted versus time t for the input pulse of relation (6) (dashed curve) and the reconstructed pulse (circles). Also plotted is the phase of the input pulse (solid curve) and of the reconstructed pulse (×'s). (b) The pulse-energy spectrum $|\tilde{E}(\omega)|^2$ plotted versus frequency ω for the input pulse of relation (6) (dashed curve) and the reconstructed pulse (circles).

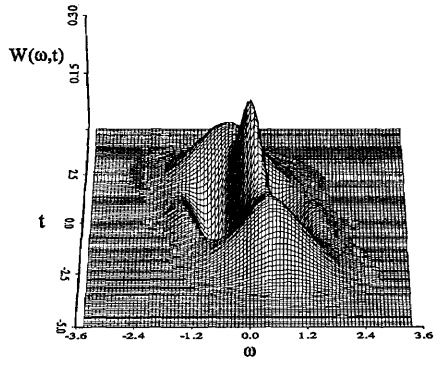

Fig. 2. The reconstructed Wigner function $W(\omega, t)$ of the pulse given by relation (6). The view is perpendicular to the frequency axis, with time increasing into the page.

in Fig. 1(a). The pulse-energy spectrum $|\tilde{E}(\omega)|^2$ is plotted in Fig. 1(b).

Using the filtered backprojection algorithm[14] for the inverse Radon transform, we have reconstructed the Wigner function using distributions $P_\theta(\omega_\theta)$ containing 128 points per rotation angle θ and 25 equally spaced angles on the interval $[-\pi/2, \pi/2]$; this reconstruction is plotted in Fig. 2. More angles and a denser sampling of ω_θ are required as τ or γ is increased. The downchirp present on the pulse is seen as the Wigner function at later times being centered at lower frequencies.

In Fig. 1 we compare the reconstructed pulse with the input pulse. The reconstruction is quite good and improves as the number of angles become larger. Increasing the number of points per angle does not significantly improve the reconstruction. Whereas the technique as demonstrated here is for theoretical data with no noise, we have used the same algorithm on real experimental data consisting of pulse quadrature amplitudes (rather than time–frequency data), and it still works quite well.[13] The algorithm is straightforward to implement.

In conclusion, the proposed technique of chronocyclic tomography can determine the amplitude and phase structure of optical pulses either for an ensemble of identical pulses or, in principle, for a single pulse (by multiplexing the spectral measurements following each pass of the multipass phase modulator). For an ensemble of nonidentical (stochastic) pulses the method yields the two time complex field correlation function. Its main advantage is that the data inversion does not require deconvolution or iterative algorithms, which are subject to error or ambiguity when the signal-to-noise ratio is not high enough. The temporal imaging system used in these measurements has the advantage that the detected field is a linear functional of the input field and thus is not subject to the same restrictions on input pulse energy and wavelength as schemes that use nonlinear devices. The method yields directly the time–frequency Wigner distribution, which has high resolution in the time–frequency domain.

We thank A. Faridani for providing the numerical algorithm used for the tomography. This research is supported by National Science Foundation grants PHY-924779 (UO) and PHY-905779 (UR).

References

1. J.-C. Diels, J. J. Fontaine, I. C. McMichael, and F. Simoni, Appl. Opt. **24,** 1270 (1985); C. Yan and J.-C. Diels, J. Opt. Soc. Am. B **8,** 1259 (1991).
2. K. Naganuma, K. Mogi, and H. Yamada, IEEE J. Quantum Electron. **25,** 1225 (1989); Appl. Phys. Lett. **54,** 1201 (1989).
3. J. L. A. Chilla and O. E. Martinez, IEEE J. Quantum Electron. **27,** 1228 (1991).
4. D. J. Kane and R. Trebino, Opt. Lett. **18,** 823 (1993).
5. E. B. Treacy, IEEE J. Quantum Electron. **QE-5,** 454 (1969).
6. B. H. Kolner and M. Nazarathy, Opt. Lett. **14,** 630 (1989).
7. M. T. Kauffman, A. A. Godil, B. A. Auld, W. C. Banyai, and D. M. Bloom, Electron. Lett. **29,** 268 (1993).
8. M. T. Kauffman, W. C. Banyai, and D. M. Bloom, in *Conference on Lasers and Electro-Optics,* Vol. 11 of 1993 OSA Technical Digest Series (Optical Society of America, Washington, D.C., 1993), paper CPD33.
9. K.-H. Brenner and K. Wodkiewicz, Opt. Commun. **43,** 103 (1982); J. Paye, IEEE J. Quantum Electron. **28,** 2262 (1992).
10. O. E. Martinez, IEEE J. Quantum Electron. **QE-23,** 59 (1987).
11. All Fourier-transform pairs will be represented by $\tilde{f}(\omega) = (2\pi)^{-1/2} \int_{-\infty}^{\infty} f(t) \exp(i\omega t) \mathrm{d}t$, where ω denotes the frequency as measured from some average carrier frequency $\overline{\omega}$. All times t and frequencies ω will be dimensionless quantities (i.e., scaled by a characteristic time T).
12. Our definition differs from that of Ref. 9 (see Ref. 13).
13. D. T. Smithy, M. Beck, A. Faridani, and M. G. Raymer, Phys. Rev. Lett. **70,** 1244 (1993).
14. G. T. Herman, *Image Reconstruction from Projections: The Fundamentals of Computerized Tomography* (Academic, New York, 1980), Chaps. 6–8, p. 90.
15. The probability distributions are normalized such that $\int_{-\infty}^{\infty} P_\theta(\omega_\theta) \mathrm{d}\omega_\theta = 1$.